

The Origin of Hindered Rotation around the Pt–N Bond in Platinum Amides

Ana C. Albéniz, Virginia Calle, Pablo Espinet,* and Sandra Gómez

Departamento de Química Inorgánica, Facultad de Ciencias, Universidad de Valladolid, Prado de la Magdalena s/n, 47005 Valladolid, Spain

Received March 23, 2001

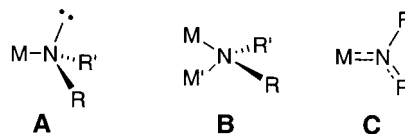
Several platinum amides of formula *trans*-[PtCl(NHAr)(PEt₃)₂] (Ar = 3-FC₆H₄, **2**; 4-FC₆H₄, **3**; 4-ClC₆H₄, **4**; 4-IC₆H₄, **5**; 4-Cl,3-NO₂-C₆H₃, **6**) have been synthesized by reaction of [PtHCl(PEt₃)₂] with aryl azides. All the complexes feature planar arylamido moieties and hindered rotation around the N-aryl and Pt–N bonds have been detected and separately studied. The X-ray crystal structures of complexes **5** and **6** have been determined. Complex **5** crystallizes in the orthorhombic space group *Pnma*, with *a* = 23.806(4) Å, *b* = 15.099(2) Å, *c* = 6.7593(10) Å, $\alpha = \beta = \gamma = 90^\circ$, and *Z* = 4. Compound **6** shows an N–H···O(NO) hydrogen bond and it crystallizes in the monoclinic space group *P2(1)/n*, with *a* = 12.215(3) Å, *b* = 8.078(2) Å, *c* = 13.052(4) Å, $\alpha = \gamma = 90^\circ$, $\beta = 90.057(6)^\circ$, and *Z* = 2. Except for Ar = 4-Cl,3-NO₂-C₆H₃, the activation energies obtained for the complexes indicate that both dynamic processes occur simultaneously with a common barrier which originates in the multiple bond character of the N-aryl bond due to a strong π -donor behavior of the N atom in the N-aryl bond. The rotation about the Pt–N bond is unfavorable because of steric congestion with the planar amide, which can be overcome only when the aromatic ring can rotate. For the complex *trans*-[PtCl{NH(4-Cl,3-NO₂-C₆H₃)}(PEt₃)₂] the barrier to rotation is mostly due to hydrogen bond interaction between the NO₂ ortho substituent and the amide H atom.

Introduction

Amido complexes are unevenly distributed among the transition metals. In contrast with the numerous and stable early transition metal compounds bearing an amido group, late transition metal amido complexes are less well represented. This is due in part to the stabilization of the M-amido bond by π -donation of the lone electron pair of the amido N to empty d orbitals in the early transition metals, which cannot occur in the late transition metals.¹ However, the number of reported amido complexes of the platinum group metals is growing.^{2–4} They are involved in the catalytic amination reactions of organic compounds that have been recently developed,⁵ and the interest in their properties and reactions has increased thereof.

The amido group single bonded to a metal has one lone pair on the N atom that makes it very nucleophilic (mode **A** in Chart 1). This lone pair is used to bind a second metal atom in bridging amido groups, which bear a tetrahedral sp³ N atom (mode **B** in Chart 1). This type of coordination is found in late transition metal complexes, especially group 10, and the dimeric complexes formed are usually very stable, the amido bridge being difficult to cleave.² Actually, dimerization may be a serious drawback in the isolation of monomeric amido complexes of the platinum group metals. Alternatively, this lone pair can get involved in the formation of π -bond, being donated to empty d orbitals in the metal (as with the early metals) or being delocalized into the R substituents, thus producing a N–M or N–R multiple bond. In this case the N atom becomes sp² hybridized (mode **C** in Chart 1).

Chart 1



Coordination mode **C** (Chart 1) is also found for group 10 transition metals and most of the monomeric derivatives fall into this type.^{2–4a,c–e,g,h,j,k,o} As suggested from the discussion above, generally the substituents on N for complexes of type **C** can delocalize electron density (R, R' = SiR₃, Ph, ...) since it is unlikely that the metal could itself contribute to this delocal-

* To whom correspondence should be sent. E-mail: espinet@qi.uva.es. Fax: 34-983-423013.

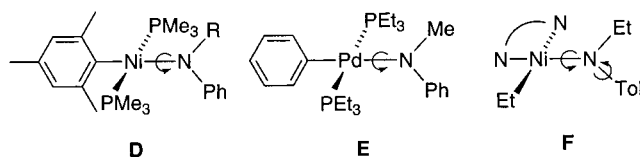
- (1) Chisholm, M. H.; Rothwell, I. P. In *Comprehensive Coordination Chemistry*; Wilkinson, G., Gillard, R. D., McCleverty, J. A., Eds.; Pergamon Press: Oxford, 1987; Vol. 2, p 176.
- (2) Fryzuk, M. D.; Montgomery, C. D. *Coord. Chem. Rev.* **1989**, *95*, 1–40.
- (3) Bryndza, H. E.; Tam, W. *Chem. Rev.* **1988**, *88*, 1163–1188.

- (4) Recent examples of monomeric Pt-group metal amido complexes: (a) Moriuchi, T.; Bandoh, S.; Miyaji, Y.; Hirao, T. *J. Organomet. Chem.* **2000**, *599*, 135–142. (b) Koo, K.; Hillhouse, G. L. *Organometallics* **1996**, *15*, 2669–2671. (c) Kim, Y.-J.; Choi, J.-C.; Osakada, K. *J. Organomet. Chem.* **1995**, *491*, 97–102. (d) Campbell, C. J.; Castañeiras, A.; Nolan, K. B. *J. Chem. Soc., Chem. Commun.* **1995**, 1939–1940. (e) Vanderlende, D. D.; Abboud, K. A.; Boncella, J. M. *Inorg. Chem.* **1995**, *34*, 5319–5326. (f) Rahim, M.; Ahmed, K. J. *Organometallics* **1994**, *13*, 1751–1756. (g) Villanueva, L. A.; Abboud, K. A.; Boncella, J. M. *Organometallics* **1994**, *13*, 3921–3931. (h) Matsunaga, P. T.; Hess, C. R.; Hillhouse, G. L. *J. Am. Chem. Soc.* **1994**, *116*, 3665–3666. (i) Rahim, M.; White, C.; Rheingold, A. L.; Ahmed, K. J. *Organometallics* **1993**, *12*, 2401–2403. (j) Schaad, D. R.; Landis, C. R. *Organometallics* **1992**, *11*, 2024–2029. (k) Villanueva, L. A.; Abboud, K. A.; Boncella, J. M. *Organometallics* **1992**, *11*, 2963–2965. (l) Glueck, D. S.; Newman Winslow, L. J.; Bergman, R. G. *Organometallics* **1991**, *10*, 1462–1479. (m) Hartwig, J. F.; Bergman, R. G.; Andersen, R. A. *J. Am. Chem. Soc.* **1991**, *113*, 6499–6508. (n) Joslin, F. L.; Johnson, M. P.; Mague, J. T.; Roundhill, D. M. *Organometallics* **1991**, *10*, 2781–2794. (o) Seligson, A. L.; Cowan, R. L.; Trogler, W. C. *Inorg. Chem.* **1991**, *30*, 3371–3381. (p) Schaad, D. R.; Landis, C. R. *J. Am. Chem. Soc.* **1990**, *112*, 1628–1629. (q) Casaluovo, A. L.; Calabrese, J. C.; Milstein, D. *J. Am. Chem. Soc.* **1988**, *110*, 6738–6744.
- (5) (a) Hartwig, J. F. *Angew. Chem., Int. Ed.* **1998**, *37*, 2046–2067. (b) Beller, M. *Angew. Chem., Int. Ed. Engl.* **1995**, *34*, 1316–1317. (c) Seligson, A. L.; Trogler, W. C. *Organometallics* **1993**, *12*, 744–751.

Table 1. M–N Distances for Some Group 10 Amido Complexes^a

complex	M–N (Å)	N–E (E = C, Si) (Å)	ref
<i>trans</i> -[Ni(Mes)(NHPh)(PMe ₃) ₂]	1.932(3)	1.354(5)	4e
<i>trans</i> -[PdPh(NHPh)(PEt ₃) ₂]	2.116(13)	1.32(2)	4g
<i>cis</i> -[PtCl(NPh ₂)(PEt ₃) ₂]	2.09(2)		9
[PtCl{N(SiMe ₃) ₂ }(COD)]	2.049(6)		2
[PdCl{N(SiMe ₃) ₂ }(tmeda)]	2.043(6)	1.700(6), 1.706(6)	4c
[PdCl{κ ³ -N(SiMe ₂ CH ₂ PPh ₂) ₂ }]	2.063(2)	1.713(2), 1.711(2)	10
<i>trans</i> -[Pt{o-C ₆ H ₄ (PPh ₂)(NH)} ₂]	2.02(1)		11
[Pd{C ₆ H ₄ C(Me)=NPh}{P(OMe) ₃ }] ₂	2.089(5)	1.371(8)	12

^a Carbamide complexes are excluded.

Chart 2

R = C(O)NHPh, C(O)NH^tBu, C(O)CHPh₂

ization. Nonetheless, some studies have proposed a π -donor contribution in the metal amido bond.⁶

The crystal structures of amido complexes of type C reported in the literature for Pd and Pt (Table 1) do not show a decrease of the distances M–N(amido) compared to the M–N(amino) distances (values of 2.103 and 2.074 Å are found for two Pt(II) complexes with primary arylamines).⁷ Only the Ni complex *trans*-[Ni(Mes)(NHPh)(PMe₃)₂] (entry 1, Table 1) shows a Ni–N(amido) distance slightly shorter than the Ni–N(amino) distance for coordinated anilines (1.932 vs. 2.06 Å respectively).^{7,8} On the other hand the M–N distances reported for those complexes (Table 1) are very close to each other and do not show significant differences; the same occurs for the N–C (or N–Si) bond lengths. Thus, the structural data suggest that the M–amido bond (M = Ni, Pd, Pt) is essentially a single bond.

In solution, hindered rotation of the amido ligand (about the M–N or N–R bonds) could be a consequence of an interaction with a bond order higher than one, but sterics can also be very important. To our knowledge, only three examples of restricted rotation about the M–N bond of group 10 amides have been reported (Chart 2).^{4e,g,h} For complexes **D** and **E** (Chart 2), the hindered rotation was detected in an indirect way, since the ortho (and meta) positions of the mesityl (**D**)^{4e} or phenyl (**E**)^{4g} groups bound to the metal were found inequivalent, which is consistent with a rigid amido ligand. The rotation of the amido group could not be studied since the only process the authors could follow was the rotation of the aryl–M bond. The different values of ΔG^\ddagger determined for complexes **D** (Chart 2) were attributed to the different rotation rates of the amido groups, although they were obtained indirectly by looking at the rotation of the mesityl group. For complex **F**, restricted rotation about the N–C(tolyl) bond and Ni–N bond were analyzed separately. Two different free energies of activation were found, the N–C rotation ($\Delta G^\ddagger = 48.9 \text{ kJ mol}^{-1}$) being easier than the Ni–N rotation ($\Delta G^\ddagger = 67.3 \text{ kJ mol}^{-1}$). The high activation barrier for this last process was assigned a steric origin.^{4h} Other examples of slow rotating amides have been found for $L_{3-n}(NR_2)_nM \equiv Mn(NR_2)L_{3-n}$

(M = Mo, W)¹³ and $L_4Os(H)(NHAr)$.¹⁴ In these cases steric effects were again deemed responsible for the restricted rotation.

In this paper we have synthesized the new aryl amido complexes of Pt(II), *trans*-[PtCl(NHAr)(PEt₃)₂] (Ar = C₆H₄X, X = 3-F, 4-F, 4-Cl, 4-I; C₆H₃XY, X = 4-Cl, Y = 2-NO₂), which show a planar structure of type C (Chart 1). We have studied the rotation about the Pt–N and N–C bond separately. From the spectroscopic data obtained, along with the crystal structure determinations for two complexes, useful information about the cause of restricted rotation around the metal amido bond can be drawn, proving that this restriction is not associated to the metal amido bond itself.

Experimental Section

General. ¹H, ¹³C, ¹⁹F, and ³¹P NMR spectra were recorded on Bruker AC-300 and ARX-300 spectrometers. Chemical shifts (in δ units, ppm) were referenced to TMS for ¹H and ¹³C, to CFCl₃ for ¹⁹F, and to H₃-PO₄ for ³¹P. The spectral data were recorded at 293 K unless otherwise noted. IR spectra were recorded using Nujol mulls on a Perkin-Elmer 883 spectrophotometer. C, H, and N elemental analyses were performed on a Perkin-Elmer 240 microanalyzer. Solvents were dried following standard procedures and distilled before use. The aromatic azides used in this work are known compounds that were prepared by the standard method starting from commercial anilines.¹⁵ [PtHCl(PEt₃)₂] was prepared as described elsewhere.¹⁶

Preparation of the Amido Complexes. Synthesis of *trans*-[PtCl(NH(*p*-I-C₆H₄))(PEt₃)₂] (5**).** To a solution of *trans*-[PtHCl(PEt₃)₂] (0.341 g, 0.73 mmol) in freshly distilled THF (15 mL) was added *p*-iodophenyl azide (0.179 g, 1.46 mmol). The mixture was stirred for 3 days at room temperature and protected from light. The brownish solution was then evaporated to dryness, and *n*-hexane (3 mL) was added to the residue. The other solid was filtered, washed with *n*-hexane (3 \times 3 mL), and air-dried: 0.447 g (89% yield). Anal. Calcd for C₁₈H₃₅ClINP₂Pt: C, 31.57; H, 5.13; N, 2.04. Found: C, 31.80; H, 4.85; N, 2.06. ³¹P{¹H} NMR (CDCl₃, δ , 121.4 MHz, 293 K), 15.96 (¹J_{Pt–P} = 2549 Hz); ¹H NMR (CDCl₃, δ , 300.13 MHz, 293 K), 7.05 (m, 2H, C₆H₄), 6.35 (b, 2H, C₆H₄), 1.75 (m, 12H, CH₂), 1.45 (b, ²J_{Pt–H} = 40 Hz, 1H, NH), 1.15 (m, 18H, CH₃). ¹H NMR (CDCl₃, δ , 300.13 MHz, 223 K), 6.12 (dd, *J* = 8.5, 2.5, 1H, H²-arom), 6.60 (dd, *J* = 8.5, 2.5, 1H, H⁶-arom), 6.94 (dd, *J* = 8.5, 2, 1H, H³-arom), 7.14 (dd, *J* = 8.5, 2, 1H, H⁵-arom), 1.80 (m, 6H, CH₂), 1.65 (m, 6H, CH₂), 1.10 (m, 18H,

(6) Poulton, J. T.; Folting, K.; Streib, W. E.; Caulton, K. G. *Inorg. Chem.* **1992**, *31*, 3190–3191.

(7) Orpen, A. G.; Brammer, L.; Allen, F. H.; Kennard, O.; Watson, D. G.; Taylor, R. J. *Chem. Soc., Dalton Trans.* **1989**, S1–S83.

(8) Even shorter bond lengths ranging from 1.819(8) to 1.889(3) Å have been reported in three-coordinated Ni complexes. Hope, H.; Olmstead, M. M.; Murray, B. D.; Power, P. P. *J. Am. Chem. Soc.* **1985**, *107*, 712–713.

(9) Eadie, D.T.; Pidcock, A.; Stobart, S. R. *Inorg. Chim. Acta* **1982**, *65*, L111–L112.

(10) Fryzuk, M. D.; MacNeil, P. A.; Rettig, S. J.; Secco, A. S.; Trotter, J. *Organometallics* **1982**, *1*, 918–930.

(11) Cooper, M. K.; Downes, J. M.; Goodwin, H. J.; MacPartlin, M.; Rosalky, J. M. *Inorg. Chim. Acta* **1983**, *76*, L155–L156.

(12) Espinet, P.; García, G.; Herrero, F. J.; Jeannin, Y.; Philoche-Levisalles, M. *Inorg. Chem.* **1989**, *28*, 4207–4211.

(13) (a) Chetcuti, M. J.; Chisholm, M. M.; Folting, K.; Maitko, D. A.; Huffman, J. C.; Janos, J. *Am. Chem. Soc.* **1983**, *105*, 1163–1170. (b) Chisholm, M. M.; Folting, K.; Huffman, J. C.; Rothwell, I. P. *Organometallics* **1982**, *1*, 251–259.

(14) Flood, T. C.; Lim, J. K.; Deming, M. A.; Keung, W. *Organometallics* **2000**, *19*, 1166–1174.

(15) Smith, P. A. S.; Boyer, J. H. *Organic Syntheses*; Wiley: New York, 1963; Collect. Vol. IV, p 75–77.

(16) Parshall, G. W. *Inorg. Synth.* **1970**, *12*, 27–29.

Table 2. Crystallographic Data for Complexes 5 and 6

	5	6
empirical formula	C ₁₈ H ₃₅ Cl ₁ N ₂ P ₂ Pt	C ₁₈ H ₃₄ Cl ₂ N ₂ O ₂ P ₂ Pt
formula weight	684.85	638.40
temperature	298(2) K	300(2) K
wavelength	0.71073 Å	0.71073 Å
crystal system	orthorhombic	monoclinic
space group	<i>Pnma</i>	<i>P2(1)/n</i>
unit cell dimensions	<i>a</i> = 23.806(4) Å, α = 90° <i>b</i> = 15.099(2) Å, β = 90° <i>c</i> = 6.7593(10) Å, γ = 90°	<i>a</i> = 12.215(3) Å, α = 90° <i>b</i> = 8.078(2) Å, β = 90.057(6)° <i>c</i> = 13.052(4) Å, γ = 90°
volume	2429.7(6) Å ³	1287.9(6) Å ³
Z	4	2
density (calculated)	1.872 Mg/m ³	1.646 Mg/m ³
absorption coefficient	7.289 mm ⁻¹	5.794 mm ⁻¹
final R indices [<i>I</i> > 2 σ (<i>I</i>)]	R1 = 0.0158, wR2 = 0.0410	R1 = 0.0440, wR2 = 0.1296
R indices (all data)	R1 = 0.0179, wR2 = 0.0419	R1 = 0.0523, wR2 = 0.1368

CH₃). ¹³C{¹H} (CDCl₃, δ , 75.4 MHz, 293 K), 157 (s, C¹), 137 (s, C³+C⁵), 117 (s, ³*J*_{Pt–C} = 58 Hz, C²+C⁶), 68.5 (s, C⁴), 12.9 (m, AA'XX' spin system, P–CH₂–CH₃, ¹*J*_{P–C} = 15 Hz), 7.7 (m, AA'XX' spin system, P–CH₂–CH₃, ²*J*_{P–C} = 5 Hz). IR, ν (N–H): 3338 cm⁻¹.

SAFETY NOTE. Aryl azides are potentially explosive. Although we did not have any problems, *great caution* should be exercised when handling these materials.

Complexes 2–4 and 6 were prepared in a similar way. The small variations on the procedure are specified in each case:

2. Molar ratio Pt/azide = 1:10; reaction time, 3 h; yield, 72%. Anal. Calcd for C₁₈H₃₅ClFNP₂Pt: C, 37.47; H, 6.11; N, 2.43. Found: C, 37.52; H, 5.71; N, 2.51. ³¹P{¹H} NMR (CDCl₃, δ , 121.4 MHz, 293 K), 15.83 (¹*J*_{Pt–P} = 2551 Hz); ¹H NMR (CDCl₃, δ , 300.13 MHz, 293 K), 6.80 (m, 1H), 6.30 (b, 2H), 5.88 (m, 1H), 1.80 (m, 12H, CH₂), 1.5 (b, 1H, NH), 1.20 (m, 18H, CH₃); ¹H NMR (CDCl₃, δ , 300.13 MHz, 223 K), **2a/2b**: 6.44/5.97 (d, ³*J*_{F–H} = 13 Hz, 1H, H²-arom), 5.86/5.88 (m, *J* = 7.5, 2 Hz, ³*J*_{F–H} = 9.5 Hz, 1H, H⁴-arom), 6.72/6.89 (q, *J* = 7.5, 7.5 Hz, ⁴*J*_{F–H} = 7.5 Hz, 1H, H⁵-arom), 6.07/6.55 (dd, *J* = 7.5, 2 Hz, 1H, H⁶-arom), 1.85 (m, 6H, CH₂), 1.65 (m, 6H, CH₂), 1.10 (m, 18H, CH₃); ¹⁹F NMR (CDCl₃, δ , 282 MHz, 223 K), –114.5 (m, **2a**), –116.8 (m, **2b**). ³¹P{¹H} NMR (CDCl₃, δ , 121.4 MHz, 223 K), 17.05 (**2a**), 16.93 (**2b**). IR: ν (N–H): 3329 cm⁻¹.

3. Molar ratio Pt/azide = 1:10; reaction time, 9 h; yield, 89%. Anal. Calcd for C₁₈H₃₅ClFNP₂Pt: C, 37.47; H, 6.11; N, 2.43; Found: C, 37.63; H, 5.75; N, 2.41. ³¹P{¹H} NMR (CDCl₃, δ , 121.4 MHz), 15.76 (¹*J*_{Pt–P} = 2586 Hz); ¹⁹F NMR (CDCl₃, δ , 282 MHz), –137.14 (m, 1F); ¹H NMR (CDCl₃, δ , 300.13 MHz, 293 K), 6.62 (t, *J* = 8.5 Hz, 2H, H³, H⁵-arom), 6.45 (b, 2H, H², H⁶-arom), 1.8 (m, 12H, CH₂), 1.60 (b, 1H, NH), 1.15 (m, 18H, CH₃); ¹H NMR (CDCl₃, δ , 300.13 MHz, 208 K), 6.70 (b, 2H, H⁶, H⁵-arom), 6.57 (b, 1H, H³-arom), 6.18 (b, 1H, H²-arom), 1.81 (b, 6H, CH₂), 1.63 (b, 6H, CH₂) 1.1 (m, 18H, CH₃). IR, ν (N–H): 3321 cm⁻¹.

4. Molar ratio Pt/azide = 1:2; reaction time, 2 days; crystallized from Et₂O; yield, 86%. Anal. Calcd for C₁₈H₃₅Cl₂NP₂Pt: C, 36.43; H, 5.94; N, 2.29. Found: C, 36.37; H, 5.57; N, 2.36. ³¹P{¹H} NMR (CDCl₃, δ , 121.4 MHz, 293 K), 15.94 (s, ¹*J*_{Pt–P} = 2558 Hz); ¹H NMR (CDCl₃, δ , 300.13 MHz, 293 K), 6.8 (b, 2H), 6.46 (b, 2H), 1.75 (m, 12H, CH₂), 1.38 (s, ²*J*_{Pt–H} = 32.7 Hz, 1H, NH), 1.15 (m, 18H, CH₃); ¹H NMR (CDCl₃, δ , 300.13 MHz, 223 K), 6.88 (dd, *J* = 8.6, 2.5 Hz, 1H, H³-arom), 6.70 (b, 2H, H², H⁴-arom), 6.21 (dd, *J* = 8.6, 3 Hz, 1H, H⁵-arom), 1.80 (m, 6H, CH₂), 1.65 (m, 6H, CH₂), 1.45 (s, 1H, NH), 1.10 (m, 18H, CH₃). IR, ν (N–H): 3327 cm⁻¹.

6. Molar ratio Pt/azide = 1:1; reaction time, 1 h; crystallized from Et₂O; yield, 70%. Anal. Calcd for C₃₆H₁₂₈N₄Cl₄O₄P₄Pt₂: C, 33.86; H, 5.33; N, 4.39. Found: C, 34.10; H, 4.95; N, 4.39. ³¹P{¹H} NMR (CDCl₃, δ , 121.4 MHz), 15.15 (s, ¹*J*_{Pt–P} = 2449 Hz); ¹H NMR (CDCl₃, δ , 300.13 MHz), 7.98 (d, *J* = 3.3 Hz, 1H, H³-arom), 7.65 (s, ²*J*_{Pt–H} = 32.6 Hz, NH, 1H), 7.31 (d, *J* = 10 Hz, 1H, H⁵-arom), 7.05 (dd, *J* = 10, 3.3 Hz, 1H, H⁶-arom), 1.65 (m, CH₂, 6H), 1.82 (m, CH₂, 6H), 1.1 (m, CH₃, 18H). IR ν (NO₂): 1539 cm⁻¹; ν (N–H) around 2900 cm⁻¹ (overlapped with the C–H stretching bands).

Determination of the Activation Parameters for the Rotation of the Amido Ligand. Variable temperature NMR spectra were recorded

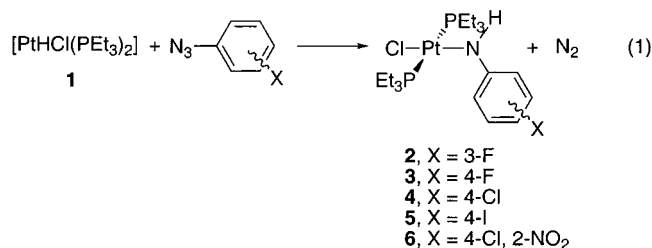
using a VT-100 temperature control unit on Bruker AC300 and ARX300 spectrometers. The temperature was calibrated by measuring the difference between the chemical shifts of MeOH signals at each temperature.¹⁷ First-order rate constants for ligand rotation (*k*_{rot}) were obtained from line shape analysis by matching the observed variable temperature ¹⁹F NMR (**2**) or ¹H NMR (**3–5**, aromatic region) spectra in CDCl₃ with those simulated using the computer programs DNMR6 (**2**) or the gNMRV3.6.5 (**3–5**).¹⁸ An Eyring plot of ln(*k*_{rot}/T) vs 1/T was represented. Activation parameters, ΔH^\ddagger and ΔS^\ddagger , were calculated from the slope and the intercept respectively of the best fit line drawn by a least-squares analysis. Uncertainties in the activation parameters were calculated from the uncertainties of the slope and the intercept of the best fit line, as reported before.¹⁹

ΔG^\ddagger values obtained from the phosphine methylene region of the ¹H NMR spectra for complexes **3–5** were determined using the Eyring equation for exchanging sites of equal population at the coalescence temperature: $\Delta G^\ddagger = 19.14T_c(9.97 + \log(T/\delta\nu))$. Errors were estimated assuming the following uncertainties in *T*_c (± 2 K) and $\delta\nu$ (± 2.5 Hz).¹⁹

X-ray Crystal Structure Determinations. Crystals were obtained by slow diffusion of *n*-hexane in a solution of **5** in acetone or by slow evaporation of a solution of **6** in a mixture of acetone and *n*-hexane. Crystals of dimensions 0.05 × 0.1 × 0.42 mm³ (**5**) or 0.05 × 0.1 × 0.16 mm³ (**6**) were mounted on the tip of glass fibers. X-ray measurements were made using a Bruker SMART CCD area-detector diffractometer. Reflections were collected, intensities integrated, and the structure was solved by direct methods procedure.²⁰ Non-hydrogen atoms were refined anisotropically and hydrogen atoms (except H(1) for both structures) were constrained to ideal geometries and refined with fixed isotropic displacement parameters. Relevant crystallographic data are contained in Table 2.

Results and Discussion

Synthesis and Structure of Complexes. Platinum amido complexes were synthesized by reaction of the hydrido complex **1** with the corresponding aryl azides, as depicted in eq 1.²¹

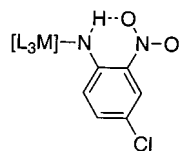


Complexes **2–5** could be isolated as yellow or ochre solids and showed a fluxional behavior in solution due to hindered

(17) Van Geet, A. L. *Anal. Chem.* **1970**, *42*, 679–6800.

(18) (a) DNMR6, *Quantum Chemical Program Exchange (QCPE 633)*; Indiana University: Bloomington, IN, 1995. (b) gNMR v 3.6.5; IvorySoft, Cherwell Scientific Publishing Ltd.: Oxford.

Chart 3



rotation of the amido ligand. Accordingly, their NMR spectra are broad at room temperature. Complex **6** is a red solid, with an apparently rigid structure in solution (unchanged ^1H and ^{31}P NMR spectra) up to 333 K.

The low-temperature spectra of complex **2** shows the presence of two atropisomers, each of them displaying the same features that will be described for **3–6**. Below their coalescence temperature complexes **3–6** showed in their $^{31}\text{P}\{^1\text{H}\}$ NMR spectra one singlet with platinum satellites, as expected for a single compound with trans stereochemistry. Their ^1H NMR spectra showed the inequivalence of all the aromatic protons, and both hydrogens of the phosphine methylene groups were diastereotopic, as expected from a rigid planar amido ligand arranged perpendicularly to the platinum coordination plane. The *NH* resonances for **2–5** appeared in the range δ 1.45–1.60, whereas for **6** it was dramatically shifted downfield (δ 7.65). Since the variations in chemical shift for the amido hydrogen are very modest when the acceptor group in para is changed from F to I, it seemed unlikely that this huge downfield shift could be due to the incorporation of a second acceptor group (NO_2) only. It appeared more reasonable that most of this effect might be due to the involvement of the *N–H* group in hydrogen bond with the ortho NO_2 substituent. This interaction should be geometrically favorable if the NO_2 and the aryl ring become roughly coplanar (Chart 3). Moreover, the shift of $\nu(\text{N–H})$ from 3338 to 3321 for complexes **2–5** to low wavenumbers (around 2900 cm^{-1} for **6**, overlapped with the *C–H* stretching bands) supported this proposal.²²

X-ray crystal structure determinations were carried out for complexes **5** and **6**. Selected bond lengths and angles are given in Table 3.

Both structures show a planar amido ligand perpendicular to the platinum coordination plane (Figure 1). The *Pt–N* distances are short, and the one found for complex **5** (2.006 \AA) is shorter than any *M–N*(amido) (*M* = Pd, Pt) bond length reported before (Table 1). The structures feature an sp^2 hybridized N atom with short *C–N* distances (closer to a *C=N* double bond distance (1.30 \AA) than to a *C–N* single bond distance (1.47 \AA)),²³ supporting that the lone pair of the N atom is heavily engaged in the formation of a multiple *C–N* bond. Not surprisingly, the distance *C–N* in complex **6** (1.31 \AA) is slightly shorter than in complex **5** (1.346 \AA), as expected from the higher acceptor character and better ability to delocalize electron density of the aryl ring in **6**. The amido hydrogen atom could be located in the Fourier map in each case. For complex **6** this confirmed the existence of $\text{N–H}\cdots\text{O}(\text{NO}_2)$ hydrogen bond ($d(\text{N}(1)\cdots\text{O}(2)) = 2.634\text{ \AA}$; $d(\text{H}\cdots\text{O}(2)) = 1.894\text{ \AA}$; $\text{O}(2)\cdots\text{H}(1)–\text{N}(1) = 130.53^\circ$). The distances found are in the range of other

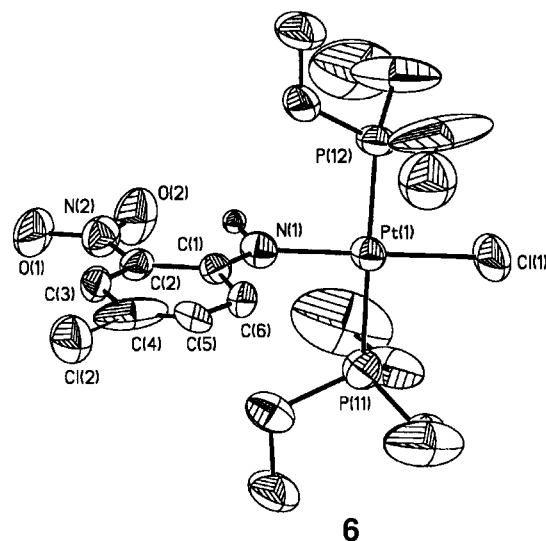
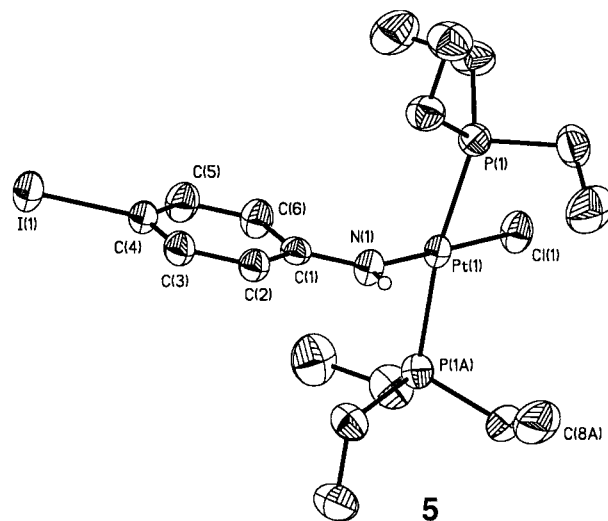


Figure 1. Molecular structures of complexes **5** and **6**.

Table 3. Selected Bond Lengths (\AA) and Angles for Complexes **5** and **6**

	5	6
Pt(1)–N(1)	2.006(4)	2.030(15)
Pt(1)–P(1)	2.3053(10)	2.322(12)
Pt(1)–P(2)	2.3053(10)	2.289(9)
Pt(1)–Cl(1)	2.3458(11)	2.297(6)
N(1)–C(1)	1.346(6)	1.31(2)
N(1)–H(1)	0.69(4)	0.97(12)
C(1)–C(2)	1.412(5)	1.46(2)
C(2)–N(2)		1.39(2)
C(4)–X(4) (X = I, 5 , Cl, 6)	2.117(4)	1.75(5)
N(1)–Pt(1)–P(1)	90.05(2)	89.9(5)
N(1)–Pt(1)–P(2)	90.05(2)	90.9(5)
N(1)–Pt(1)–Cl(1)	179.29(12)	176.8(5)
C(1)–N(1)–Pt(1)	126.9(3)	129.2(12)
N(1)–C(1)–C(6)	123.0(4)	121.8(15)
N(1)–C(1)–C(2)	121.0(4)	126.0(15)
O(2)–H(1)–N(1)		126.0(15)

intramolecular $\text{N–H}\cdots\text{O}$ hydrogen bonded structures reported in the literature for coordinated ligands²⁴ and also for β -enamiones with comparable H-bonded six-membered structures.²² The H-bond is bent but this is probably imposed by the geometry of the molecule.

(19) (a) Casado, A. L.; Casares, J. A.; Espinet, P. *Organometallics* **1997**, *16*, 5730–5736. (b) Kirkup, L. *Experimental Methods*; Wiley: Brisbane, 1994.

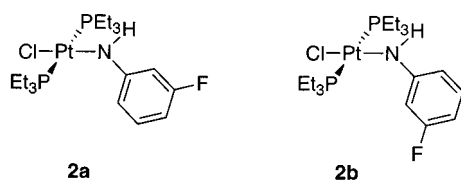
(20) The data analysis and the drawing were performed with the following programs: SMART V5.051, 1998; SAINT V6.02, 1999. Sheldrick, G. M. *SHELXTL V5.1*; Bruker AXS, Inc.: Madison, WI, 1998.

(21) Beck, W.; Bauder, M. *Chem. Ber.* **1970**, *103*, 583–589.

(22) Gilli, P.; Bertolasi, V.; Ferretti, V.; Gilli, G. *J. Am. Chem. Soc.* **2000**, *122*, 10405–10417.

(23) Emsley, J. *The Elements*; Clarendon Press: Oxford, 1991.

Chart 4

**Table 4.** Activation Parameters for the Rotation of the Amido Ligand about the N-aryl Bond in Complexes 2–5^a

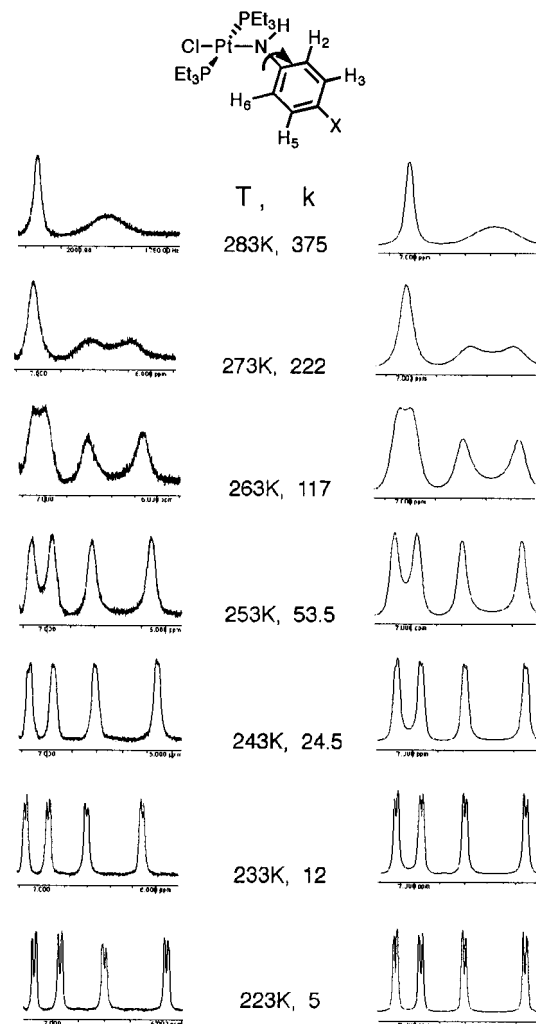
complex	ΔS^\ddagger (J mol ⁻¹ K ⁻¹)	ΔH^\ddagger (kJ mol ⁻¹)	ΔG_{298}^\ddagger (kJ mol ⁻¹)
2	-13 ± 4	49.1 ± 1.2	53.0 ± 1.7
3	-32 ± 5	33.3 ± 1.1	42.8 ± 1.5
4	-68 ± 6	32.3 ± 1.4	53 ± 1.8
5	-69.2 ± 1.9	35.7 ± 0.5	56.3 ± 0.6

^a Data obtained by line shape analysis of ¹H (3–5) or ¹⁹F (2) NMR signals.

Fluxional Behavior of the Complexes. The substitution of the aryl ring in the meta or ortho positions, as in complexes 2 and 6, can give rise to atropisomers by restricted rotation around the N-aryl bond. In fact, the NMR spectra of complex 2 (CDCl₃) in the slow exchange limit (223 K) revealed a mixture of two isomers in a ratio 2a/2b = 1:0.7 (Chart 4). Two signals were observed in the ³¹P{¹H} (δ 17.05, s, $J_{\text{Pt-P}} = 2504$ Hz; and 16.93, s, $J_{\text{Pt-P}} = 2520$ Hz) and ¹⁹F (δ -114.46, m; -116.77, m) spectra. The ¹H spectrum showed clearly two sets of aromatic signals (two rotamers) and two groups of methylene protons from the PEt₃ ligands each showing that the two H atoms on each methylene group are diastereotopic. When the temperature was raised all the methylenic hydrogen atoms became isochronous. This requires fast rotation about both the N-aryl and the Pt–N bonds. Using the ¹⁹F NMR data, line shape analysis was carried out which gave the rate of exchange at different temperatures and, by using an Eyring plot, the activation parameters collected in Table 4. Although 2 does not allow to study the rotation about the N-aryl bond independently, these activation parameters are similar to those found for the rotation about the N-aryl bond in 2–5, which were assigned as discussed below.

The analysis of the NMR spectra of the complexes with para substituted amido ligands (3–5) at variable temperature in CDCl₃ turned out to be very informative. Restricted rotation does not produce atropisomers in this case, but different changes in the spin systems for the ¹H NMR spectra of these derivatives are expected depending on the motion involved. Fast rotation about the Pt–N bond should produce equivalence of the methylenic H atoms only. Fast rotation around the N-aryl bond should bring about equivalence of the aryllic hydrogen atoms only. Thus, both movements can be studied independently by looking at the corresponding signals separately.

Figure 2 shows the change in the aromatic region of the spectrum for complex 5 as the temperature increases. Rotation about the N-aryl bond is the only process required to bring about the coalescence of both ortho protons on one side and both meta protons on another, and this movement certainly does not require any other modification in the molecule (such as rotation around the Pt–N bond). Line shape analysis at different temperatures

**Figure 2.** Real (left) and simulated (right) ¹H NMR spectra of the aromatic region at variable temperature for complex 5.

(Figure 2) was carried out and an Eyring plot led to the activation parameters for the rotation about the N-aryl bond of the ligand (Table 4).

The free energies of activation found are also similar to the data reported for restricted rotation about the C–N bond in aromatic amines (cf. $\Delta G_{\text{rot}(201.5 \text{ K})}^\ddagger = 44.3$ kJ mol⁻¹ for 4-ClC₆H₄NMe₂ and $\Delta G_{\text{rot}(201.5 \text{ K})}^\ddagger = 46$ kJ mol⁻¹ for 4),²⁵ and in the Ni complex [Ni(bipy)(Et)(NEtToI)] (N–C(tolyl)) $\Delta G_{\text{rot}}^\ddagger = 48.9$ kJ mol⁻¹).^{4h}

On the other hand, the two protons of the methylene groups of the phosphines become equivalent only when the platinum coordination plane becomes a symmetry plane, which requires rotation of the amido group about the N–Pt bond (Figure 3). Provided that rotation about the N-aryl bond were not required, the free energies of activation obtained looking at this region in the spectra should correspond to ΔG^\ddagger for the rotation about the Pt–N bond. Table 5 collects the thermodynamic data obtained for complexes 3–5. There is a perfect coincidence (within the experimental error) between the ΔG^\ddagger values for rotation about the N-aryl bond and those for rotation about the Pt–N bond. This suggests that the rotation around the Pt–N bond does require simultaneous rotation around the N-aryl bond, which is the highest barrier and becomes rate determining for

(24) Some recent examples: (a) Moriuchi, T.; Watanabe, T.; Ikeda, I.; Ogawa, A.; Hirao, T. *Eur. J. Inorg. Chem.* **2001**, 277–287. (b) Sakagami-Yoshida, N.; Teramoto, M.; Hioki, A.; Fuyuhiko, A.; Kaizari, S. *Inorg. Chem.* **2000**, 39, 5717–5724. (c) Cini, R.; Grabner, S.; Bukovec, N.; Cerasino, L.; Natlie, G. *Eur. J. Inorg. Chem.* **2000**, 1601–1607. (d) Castarnelas, R.; Esteruelas, M. A.; Oñate, E. *Organometallics* **2000**, 19, 5454–5463.

(25) Oki, M. *Applications of Dynamic NMR Spectroscopy to Organic Chemistry; Methods in Stereochemical Analysis 4*; VCH Publishers: New York, 1985; pp 86–87.

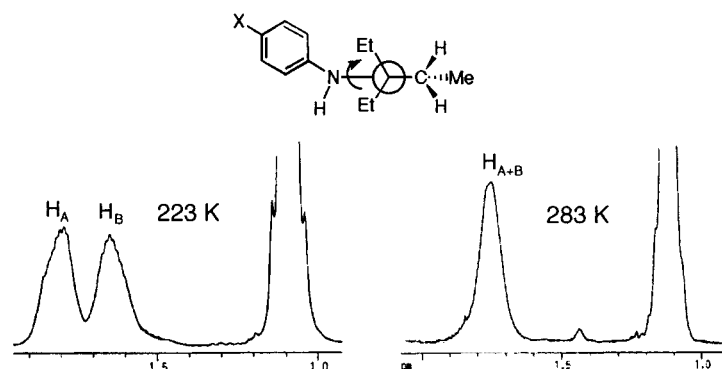


Figure 3. Variable temperature ^1H NMR spectra of complex **5** in the methylene region.

Table 5. Free Energies of Activation for the Rotation about the N-aryl and Pt–N Bonds for complexes **3–5**

complex	T_{coal} (K)	$\Delta G_{\text{rot(Pt-N)}}^{\ddagger}$ (kJ/mol) ^a	$\Delta G_{\text{rot(C-N)}}^{\ddagger}$ (kJ/mol) ^b
3	223	44.58 ± 0.43	40.4 ± 1.6
4	248	50.64 ± 0.44	49 ± 2
5	258	53.07 ± 0.45	53.6 ± 1.7

^a Obtained by analysis of the phosphine methylene region of the ^1H NMR spectra. ^b Obtained by analysis of the aromatic region of the ^1H NMR spectra.

the whole process (see Conclusions). This is in contrast with the results reported for $[\text{Ni}(\text{bipy})(\text{Et})(\text{NEtTol})]$ where the free energies of activation found for rotation about the N–C (48.9 kJ mol^{-1}) and Ni–N (67.3 kJ mol^{-1}) are very different and indicate that both processes are independent.^{4h} Since the Et substituent on the amido ligand of the Ni complex increases the steric hindrance in that case, rotation about the N–C(Tolyl) bond is not sufficient and the Ni–N barrier for rotation is higher than the energy needed for rotation about the Pt–N bond of complexes **2–5**.

Other alternative mechanisms for rotation about the N-aryl and Pt–N bonds were considered and discarded. The dynamic processes are intramolecular and the rates do not increase with the concentration of the complex, which rules out any bimolecular mechanism. The polarity of the solvent does not influence the process either, and no change in rate was observed when complex **5** was dissolved in a CDCl_3 solution of $(\text{NBu}_4)\text{-PF}_6$, which discards the dissociation of the amido ligand to form an ionic pair as an alternative mechanism. The involvement in the rotation in an amino ligand (formed by the presence of traces of acid) or an imino complex (by deprotonation of the amido ligand) was excluded since the addition of CaH_2 to a solution of **5** in CDCl_3 does not affect the rotation rate.

Finally, no fluxional behavior was observed for complex **6** up to 333 K. Only one atropisomer with diastereotopic methylenic hydrogen atoms was observed in solution, suggesting that the hydrogen bonding observed in the solid state, which is preserved in solution, precludes the necessary rotation about the N-aryl bond.

Conclusions

The barrier observed for complexes **2–5** corresponds to that of the rotation about the N-aryl bond, which is electronic in origin and reflects the multiplicity of the bond. In effect, the rotational barrier can be associated to the accessibility of a transition state similar to **A** in Chart 1, with a lone electron pair on a sp^3 N atom.

The rotation about the Pt–N bond is probably a low energy process in the absence of steric considerations, but a planar amido group with a sp^2 N atom should clash with the phosphines (Figure 4a). This steric problem can be overcome when rotation

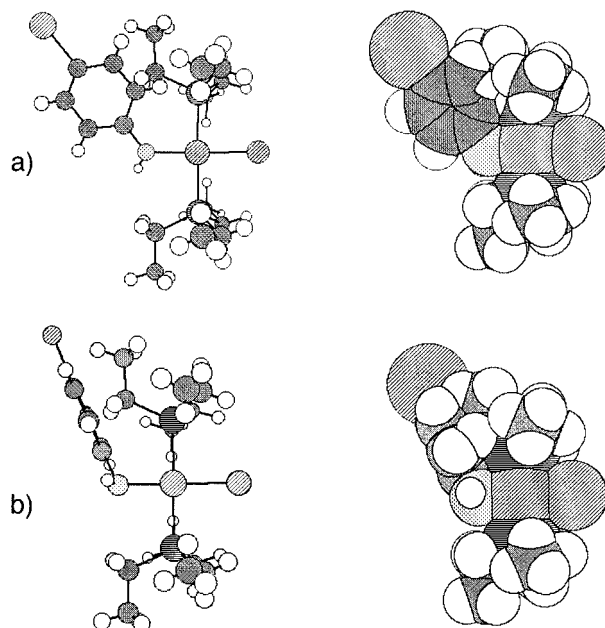


Figure 4. Ball and stick and space filling models of the partial rotation about the Pt–N bond for (a) a rigid amido moiety and (b) an amido ligand after rotation about the C–N bond.

about the N-aryl bond occurs and the hybridization of N changes in the transition state from sp^2 to sp^3 and the phenyl ring can, by N-aryl rotation, relieve the steric hindrance that the planar arrangement was imposing (Figure 4b). There is no need to invoke any multiple character of the Pt–N bond.

The rigidity of complex **6** indicates a much higher barrier for the rotation around the N-aryl bond. Two effects should contribute to make this barrier higher than for any other compound in this study: (i) the aryl ring in **6** bears two electron acceptor groups and should produce the N-aryl bond with the highest multiplicity; (ii) the hydrogen bond must be broken. Considering the more modest range of variations in $\Delta G_{\text{rot}}^{\ddagger}$ produced upon changes of the withdrawing group in **2–5**, it seems that most of the dramatic increase in $\Delta G_{\text{rot}}^{\ddagger}$ observed for **6** must be attributed to the hydrogen bond.

Acknowledgment. We thank the Dirección General de Enseñanza Superior (Ministerio de Educación y Cultura, PB96-0363) and the Junta de Castilla y León (VA80/99 and VA17/00B)f or financial support.

Supporting Information Available: Crystallographic data, in CIF format. This material is available free of charge via the Internet at <http://pubs.acs.org>.